Available online at www.sciencedirect.com

SCIENCE DIRECT®

Inorganica Chimica Acta 346 (2003) 187–196

Inorganica Chimica Acta

www.elsevier.com/locate/ica

Crystal structures and luminescent properties of terbium(III) carboxylates

Beatriz Barja [a], Ricardo Baggio [b], Maria T. Garland [c], Pedro F. Aramendia [a], Octavio Peña [d], Mireille Perec [a,*]

[a] Departamento de Química Inorgánica, Analítica y Química Física, Facultad de Ciencias Exactas y Naturales, INQUIMAE, Universidad de Buenos Aires, Ciudad Universitaria, Pabellón II, 1428 Buenos Aires, Argentina

[b] Departamento de Física, Comisión Nacional de Energía Atómica, Avda del Libertador 8250, 1429 Buenos Aires, Argentina

[c] Departamento de Física, Facultad de Ciencias Físicas y Matemáticas, Universidad de Chile, Avda. Blanco Encalada 2008, Casilla 487-3, Santiago, Chile

[d] U.M.R. 6511, L.C.S.I.M. CNRS, Université Rennes I, 35042 Rennes, France

Received 17 August 2002; accepted 18 October 2002

Abstract

Single crystals of three terbium(III) carboxylates of formulae $[Tb_2(CH_3COO)_6(H_2O)_4]\cdot 4H_2O$ (**1**), $[Tb_2(CF_3COO)_6(H_2O)_6]$ (**2**) and $[Tb(Hoda)_3]\cdot H_2oda\cdot H_2O$ (**3**) ($H_2oda = 2,2'$-oxydiacetic acid) were obtained and their structures determined by X-ray crystallography. Compounds **1** and **2** are dimeric, in the former the terbium atoms are bound by two tridentate carboxylates in the μ_2-bridging mode, whereas in the latter the bridging is fourfold with all carboxylates in the *syn–syn* coordination mode. Compound **3** is mononuclear containing three tridentate Hoda anions, and consecutive units are linked by a network of H-bonds involving the interstitial molecules. The luminescence spectra of the carboxylates were analyzed in the solid state and in aqueous solution. Comparison of the emission lifetimes in H_2O and D_2O allowed the determination of the average value for q, the number of coordinated water molecules, being 9.2 for **1** and **2** and 3.6 for **3**, respectively. The quenching effect of Cu(II) on the luminescence of the terbium(III) carboxylates was evaluated through the emission decay constants. From the addition of Cu(II) to an aqueous solution of **3**, single crystals of polymeric $[\{Cu_3Tb_2(oda)_6(H_2O)_6\}\cdot 12H_2O]_n$ (**4**) were isolated with completely quenched luminescence. Compound **4** exhibits an overall antiferromagnetic interaction.

Keywords: Crystal structures; Terbium(III) carboxylates; Luminescence

1. Introduction

Rare earth carboxylates show an intriguing variety of crystal structures due to the usually high coordination number of the metal ions and to the many types of coordination of the carboxylate ligands in the complexes. Dimeric and polymeric forms are most frequently observed for these compounds [1–4]. Rare-earth carboxylates can be used as starting materials in a wide range of applications in materials science including superconductors, magnetic materials, catalysts and luminescent probes [5–10]. In particular, probes based on Eu(III) and Tb(III) carboxylates are of special relevance because of the cations long-lived excited states $^5D_0$ and $^5D_4$, respectively.

The crystal structures of dimeric europium acetate [11], polymeric europium acetate [12], and dimeric trifluoroacetate [13] have been reported. Recently, we have isolated two europium carboxylates, $[\{Eu_2(oda)_3(H_2O)_2\}\cdot 5H_2O]_n$ and $[Eu(oda)(Hoda)(H_2O)]\cdot 2H_2O$ (oda = oxydiacetate), by adjusting the pH value of the reaction mixture [14].

Since the particular properties of lanthanide carboxylates in general are related to their structures, the detailed study of the factors influencing structure and variations along the lanthanide series is of interest. Herein, we report the structures and properties of

* Corresponding author. Tel.: +54-11-4576 3358; fax: +54-11-4576 3341.

E-mail address: perec@g1.fcen.uba.ar (M. Perec).

0020-1693/03/$ - see front matter © 2002 Elsevier Science B.V. All rights reserved.
PII: S0020-1693(02)01429-9

dimeric $[Tb_2(CH_3COO)_6(H_2O)_4]\cdot 4H_2O$ and $[Tb_2(CF_3COO)_6(H_2O)_6]$ and of mononuclear $[Tb(Hoda)_3]\cdot H_2oda\cdot H_2O$. Their luminescence behavior in solid and aqueous solution state is described. While analyzing the quenching effect of Cu(II) on the fluorescence of the Tb(III) carboxylates in aqueous solution, well shaped crystals of heterometallic $[\{Cu_3Tb_2(oda)_6(H_2O)_6\}\cdot 12H_2O]_n$ were isolated, and its full characterization is included in this study.

2. Experimental

2.1. Materials and methods

All chemicals were reagent-grade purity purchased from Aldrich and used as received. Water was purified by a Millipore Milli-Q system. Elemental Analyses (C, H) were performed on a Carlo–Erba EA 1108 instrument. Copper was determined on a Shimadzu AA6501 spectrophotometer. IR spectra were recorded on a Nicolet FT-IR 510 P spectrophotometer using the KBr pellet technique. Thermogravimetric analyses were recorded on a Shimadzu DTG50 thermal analyzer under an atmosphere of air at a heating rate of 5 °C min^{-1}. Powder X-ray diffraction (XRD) were collected using monochromated Cu Kα radiation on a Philips X'Pert diffractometer. Temperature dependent magnetic susceptibilities of compound **4** were recorded on a SHE 906 SQUID susceptometer in the range 2–300 K with an applied field of 500 G. Pascal's constants were used to estimate the correction for the underlying diamagnetism of the sample [15].

2.2. Preparations

2.2.1. $[Tb_2(CH_3COO)_6(H_2O)_4]\cdot 4H_2O$ (*1*)

Terbium acetate tetrahydrate (0.200 g) was recrystallized from 25 ml of a water–EtOH (1:1 v/v) solution. Colorless crystals suitable for X-ray diffraction were isolated after a week and dried in vacuum. *Anal*. Calc. for $C_{12}H_{34}O_{20}Tb_2$: C, 17.65; H, 4.20. Found: C, 17.70; H, 4.20%. Main FT IR bands (KBr, cm^{-1}): 1541(vs), 1457(vs), 1417(vs), 1384(vs), 1318(m), 1051(m), 1025(m), 964(m), 944(m), 683(s), 611(m), 474(w). The TGA diagram shows a weight loss of 17.3% in overlapping steps in the range 89–167 °C which corresponds to the simultaneous loss of the water of crystallization and coordination, calc. 17.5%.

2.2.2. $[Tb_2(CF_3COO)_6(H_2O)_6]$ (*2*)

Trifluoroacetic acid (0.70 g, 6.0 mmol) was added slowly to 10 ml of a solution of terbium acetate tetrahydrate (0.35 g, 1 mmol) kept in an ice bath. The reaction mixture was allowed to warm to room temperature (r.t.) and maintained with stirring for 2 h. The resulting solution was filtered and allowed to stand in a stoppered flask for 1 week. A colorless solid separated, which was washed with a small amount of ice water, filtered and dried in vacuum. Yield: 0.40 g, 80%. *Anal*. Calc. for $C_{12}H_{12}F_{18}O_{18}Tb_2$: C, 13.05; H, 1.10. Found: C, 13.10; H, 1.10%. Main FT IR bands (KBr, cm^{-1}): 1726(vs), 1668(vs), 1623(vs), 1473(m), 1459(m), 1384(m), 1208(vs,ν_{CF3}), 1152 (vs,ν_{CF3}), 799(s), 730(s), 721(s), 606(w), 523(m). The TGA diagram shows a weight loss of 9.6% in the range 90–130 °C which corresponds to the six-coordinated water molecules, calc. 9.8%. The compound is highly hygroscopic; its high moisture sensitivity restricted further studies of the solid. However, spectroscopic and crystal structure determination was successfully accomplished by the usual techniques.

2.2.3. $[Tb(Hoda)_3]\cdot(H_2oda)\cdot(H_2O)$ (*3*)

Terbium acetate tetrahydrate (0.40 g, 1 mmol) and oxydiacetic acid (0.80 g, 6 mmol) were dissolved in water (50 ml) and the solution was refluxed under stirring for 3 h and passed through a glass filter. The filtrate was stored at pH 5 in a stoppered flask at r.t. for a week, whereupon colorless crystals of the product were collected by filtration and dried in air. Yield: 0.40 g, 55%. *Anal*. Calc. for $C_{16}H_{23}O_{21}Tb$: C, 27.05; H, 3.25. Found: C, 27.00; H, 3.25%. Main FT IR bands (KBr, cm^{-1}): 1739(vs), 1718(vs), 1679(vs), 1644(vs), 1449(m), 1426(m), 1402(w), 1276(m), 1245(m), 1237(m), 1218(m), 1146(vs), 1118(vs), 1050(s), 1017(w), 1008(w), 911(m), 883(w), 691(m), 598(m). TGA analysis shows that thermal degradation occurs in overlapping steps in the range 50–800 °C. The mass of the final product corresponds to the complete combustion to cubic Tb_4O_7, as shown by the XRD diagram [16].

2.2.4. $[\{Cu_3Tb_2(oda)_6(H_2O)_6\}\cdot 12H_2O]_n$ (*4*)

Crystals of compound **4** were isolated from the addition of copper acetate to a solution of compound **3**. The heterometallic compound is isostructural with the reported compounds $[\{Cu_3Ln_2(oda)_6(H_2O)_6\}\cdot 12H_2O]_n$ for Ln = Y, Gd, Eu, Nd and Pr [17]. *Anal*. Calc. for $C_{24}H_{60}Cu_3O_{48}Tb_2$: C, 17.70; H, 3.70; Cu, 11.70. Found: C, 17.75; H, 3.70; Cu, 11.50%. Main FT IR bands (KBr, cm^{-1}): 1594(vs), 1476(s), 1440(vs), 1368(m), 1316(vs), 1248(w), 1127(s), 1060(s), 970(m), 944(m), 625(s,br).

2.3. X-ray crystallography

A summary of crystal parameters, data collection and refinement details is given in Table 1 and structural parameters in Table 2. Data were collected on a Bruker SMART 6000 diffractometer equipped with a CCD detector and graphite-monochromated Mo Kα (λ = 0.71073 Å) radiation. The unit cell parameters were determined by least-squares refinement of the whole, highly redundant data set ($2\theta \leq 50°$) collected by the Ω-

Table 1
Crystallographic data for compounds **1**–**4**

	1	2	3	4
Empirical formula	$C_6H_{17}O_{10}Tb$	$C_6H_6F_9O_9Tb$	$C_{16}H_{23}O_{21}Tb$	$C_{24}H_{60}Cu_3O_{48}Tb_2$
Formula weight	408.12	552.03	710.26	1625.18
Crystal system	triclinic	monoclinic	monoclinic	hexagonal
Space group	$P\bar{1}$ (no. 2)	$P2_1/c$ (no. 14)	$P2_1/n$ (no. 14)	$P6/mcc$ (no. 192)
Crystal color	colorless	light yellow	colorless	blue
a (Å)	8.897(2)	9.160(1)	6.540(1)	14.693(2)
b (Å)	9.280(2)	18.828(1)	25.099(4)	14.693(2)
c (Å)	10.460(2)	9.751(1)	14.618(2)	15.125(2)
α (°)	91.70(3)	90	90	90
β (°)	114.00(3)	113.94(1)	93.04(1)	90
γ (°)	118.18(3)	90	90	120
V (Å^3)	668.6(2)	1537.1(1)	2396.1(6)	2827.6(7)
Z	2	4	4	2
D_{calc} (g cm^{-3})	2.03	2.38	1.97	1.91
μ(Mo Kα) (mm^{-1})	5.33	4.74	3.05	3.69
F(000)	396	1040	1408	1610
Crystal size (mm)	0.24 × 0.22 × 0.16	0.42 × 0.30 × 0.24	0.34 × 0.12 × 0.08	0.34 × 0.32 × 0.14
Max./min. transmission	0.38, 0.33	0.28, 0.22	0.74, 0.53	0.68, 0.56
Reflections (collected, unique, R_{int})	3964, 2796, 0.013	8889, 3418, 0.029	14 186, 5385, 0.089	14 793, 1137, 0.056
R_1 [a], wR_2 [b] [$F^2 > 2\sigma(F^2)$]	0.020, 0.055	0.024, 0.059	0.064, 0.128	0.027, 0.077
Goodness-of-fit on F^2	1.052	0.950	0.928	1.151
Final $\Delta\rho$ (e Å^{-3})	0.706, −0.671	0.838, −1.050	1.285, −1.527	0.753, −0.390

Absorption correction: semi-empirical (SADABS, Bruker 2000).
[a] R_1: $\Sigma\,||F_o|-|F_c||/\Sigma\,|F_o|$.
[b] wR_2: $[\Sigma\,[w(F_o^2-F_c^2)^2]/\Sigma\,[w(F_o^2)^2]]^{1/2}$.

scan technique and corrected for Lorentz and absorptions effects (ψ-scan). The fluorine atoms of all terminal CF_3 groups in compound **2** were found to be disordered over three different rotational orientations, and were refined in each ligand as three independent CF_3 rigid groups. This model gave a fairly flat final difference Fourier map. The starting model used for structure resolution of compound **3** was the one reported for the isostructural [{Gd(Hoda)$_3$}·(H_2oda)·(H_2O)] [18]. As reported previously for other members of the series [17], the hydration content of **4** was variable, and a satisfactory correlation between the analytical data and the occupancy values from refinement was obtained from single crystals dried in air. Refinement was performed by full-matrix least-squares in F^2, with anisotropic thermal parameters for the non-hydrogen atoms. Computer programs used in this study were the SHELXL-97, and SHELXLTL/PC software packages [19,20].

2.4. Photophysical measurements

The luminescence emission spectra of the compounds were recorded on a PTI QuantaMaster QM-1 luminescence spectrometer. Solid samples were placed between quartz plates and their luminescence was measured in a 30° front face geometry, detecting the emission from the back face. Excitation wavelength was 369 nm in all cases. Liquid samples were placed in a 1 cm square quartz fluorescence cell and measured in right angle geometry. Excitation and emission bandwidths were set to 4 and 1 nm for the solid and 4 and 2 nm for the liquid samples, respectively.

Luminescence lifetimes in solid state and in D_2O or H_2O were measured in the same geometry as described for steady state spectra. Samples were excited at 354 nm with a frequency tripled Nd:YAG laser (Spectron), which delivered pulses of 30 mJ, 8 ns FWHM at 10 Hz. Emitted light passed through a monochromator and was detected at 488 and 544 nm with 4 nm bandwidth. Light was detected with a R928 Hammamatsu photomultiplier, amplified (SR.445, Stanford Research System) and the transient signal was averaged in a HP54502 digital oscilloscope and stored in a PC AT486. The traces were fitted to a single exponential decay and the goodness-of-fit was judged by an homogeneous time-distribution of residuals.

3. Results and discussion

3.1. Crystal structures

The crystal structure of **1** consists of dimeric units related by an inversion center as shown in Fig. 1. The two Tb(III) metal ions are linked by two bridging tridentate carboxylate groups (one of the carboxylate oxygen atoms in the acetate anion is bound to two Tb

Table 2
Selected bond lengths (Å) for compounds **1**–**4** [a]

1			
Tb–O(1W)	2.343(3)	C(1A)–O(1A)	1.260(4)
Tb–O(2W)	2.360(2)	C(1A)–O(2A)	1.262(4)
Tb–O(2B)^{i}	2.378(2)	C(1B)–O(1B)	1.248(4)
Tb–O(2C)	2.412(3)	C(1B)–O(2B)	1.266(4)
Tb–O(2A)	2.433(2)	C(1C)–O(1C)	1.256(4)
Tb–O(1B)	2.449(3)	C(1C)–O(2C)	1.259(4)
Tb–O(1A)	2.465(3)		
Tb–O(1C)	2.470(2)		
Tb–O(2B)	2.567(2)		
2			
Tb–O(1A)	2.332(2)	C(1A)–O(1A)	1.234(4)
Tb–O(2C)^{ii}	2.334(2)	C(1A)–O(2A)	1.239(4)
Tb–O(2A)^{ii}	2.359(2)	C(1B)–O(2B)	1.216(4)
Tb–O(1B)	2.366(2)	C(1B)–O(1B)	1.248(4)
Tb–O(2W)	2.372(3)	C(1C)–O(2C)	1.222(4)
Tb–O(1W)	2.398(3)	C(1C)–O(1C)	1.250(4)
Tb–O(3W)	2.420(2)		
Tb–O(1C)	2.442(2)		
3			
Tb–O(1A)	2.330(6)	C(1B)–O(1B)	1.201(10)
Tb–O(1B)	2.365(6)	C(1B)–O(2B)	1.278(11)
Tb–O(1C)	2.397(6)	C(4B)–O(4B)	1.233(10)
Tb–O(3A)	2.458(6)	C(4B)–O(5B)	1.262(10)
Tb–O(3B)	2.435(5)	C(1C)–O(1C)	1.219(10)
Tb–O(3C)	2.571(6)	C(1C)–O(2C)	1.310(10)
Tb–O(5A)	2.328(7)	C(4C)–O(5C)	1.226(11)
Tb–O(5B)	2.395(6)	C(4C)–O(4C)	1.274(10)
Tb–O(5C)	2.286(6)	C(1D)–O(1D)	1.194(11)
C(1A)–O(1A)	1.235(10)	C(1D)–O(2D)	1.300(11)
C(1A)–O(2A)	1.284(10)	C(4D)–O(5D)	1.198(12)
C(4A)–O(4A)	1.225(12)	C(4D)–O(4D)	1.309(12)
C(4A)–O(5A)	1.261(14)		
4			
Tb–O(1)	2.393(2)	O(1)–C(1)	1.249(3)
Tb–O(3)	2.471(3)	O(2)–C(1)	1.247(3)
Cu–O(2)	1.951(2)		
Cu–O(1W)	2.500(4)		

[a] Symmetry codes: (i) $-x$, $-y+2$, $-z$; (ii) $-x+1$, $-y+1$, $-z+1$.

atoms, whereas the second oxygen atom is bound directly to a Tb atom). As a result the two oxygen atoms (O2B) and O(2B′) which are bound in a μ_2-bridging manner to both terbium ions form a monoatomic bridge. Due to the inversion center, the TbO(2B)Tb′(O2B′) network is perfectly planar. The two TbO9 coordination polyhedra are best described as distorted TCTP. The Tb–O(aqua) distances are 2.343(3) and 2.360(2) Å, the shortest in the polyhedra, whereas Tb–O(carboxylate) distances display a rather broad span: 2.378(2)–2.5677(2) Å. The resulting Tb···Tb intradimer separation is 4.190(1) Å, and the next shortest distance between Tb centers is 6.218(1) Å. The bonding between dimers is through H-bonds, Fig. 2. All hydrate H-atoms are involved in medium to weak hydrogen bonds, Table 3. Compound **1** is isostructural with the reported acetate tetrahydrates with Eu [21], Gd [22], Ho [23] and Er [24].

The crystal structure of **2** consists of binuclear centrosymmetric dimers, the carboxylate bridging here is fourfold and in the *syn–syn* coordination mode. Three aqua molecules and one monodentate trifluoroacetato group complete eight-coordination polyhedra at each metal, Fig. 3. The compound is isostructural to the homologous Pr [25], Eu [26], Gd [27] and Dy [28] trifluoroacetates. Four of the Tb–O(carboxylate) distances are within the narrow range of 2.332(2)–2.366(2) Å, whereas the fifth one Tb–O(1C) of 2.442(2) Å departs significantly from the average value. The Tb–O(aqua) distances in the range 2.372(2)–2.420(2) Å are somewhat larger than those found in **1**. The fourfold carboxylate bridge in this compound leads to a Tb···Tb intradimer separation of 4.466(1) Å. The change of CH_3COO^- for the powerful Lewis acid CF_3OOO^-, brings about several changes in the structure: (i) the number of coordination and crystallization water molecules are different; and (ii) the coordination number of the Tb(III) ions and the carboxylate bonding modes are different too. As a result the intradimer Tb···Tb distance increases by approximately 0.50 Å. Similar changes have been reported for the related pairs of Eu(III) and Gd(III) compounds. Significant H-bonds involve the aqua molecules and the oxygen atoms of the trifluoroacetate ligands. One of these, O1W–H1WA···O2B, is intramolecular, linking O2B to the rest of molecule. The H-bond O3W–H3WA···O1C provides the link for a linear array running parallel to the crystallographic *a* axis, and is likely to be responsible for the weakening of the Tb–O1C bond. The remaining hydrogen bond (O2W–H2WA···O2B[x, $-y+1/2$, $z-1/2$]) together with other weak H···F interactions provide to the interchain cohesion, Table 3 (Fig. 4).

The crystal structure of **3** consists of monomeric units of $[Tb(C_4H_5O_5)_3]$ with a free oxydiacetic acid and a water molecule as solvates, Fig. 5. The terbium ion shows a ninefold coordination to three tridentate Hoda anions, in the classical TCTP scheme. In spite of the lack of internal symmetry of the coordination polyhedron, the bond distances define two sets of values. One set consists of six short capping bonds with a mean value of 2.35(4) Å and three equatorial bonds with a mean value of 2.49(7) Å. Hydrogen-bonding interactions in **3** define the complex packing scheme illustrated in Fig. 6. On one side the Tb coordination polyhedra form columns parallel to the crystallographic *a* axis, through the hydrogen interactions in the O=C–OH groups. These chains are in turn connected both, the free acid as well as the water molecules, to define a broad solvent strip limited at both sides by columns of Tb polyhedra. These strips evolve along *a* and pile up in the *b* direction

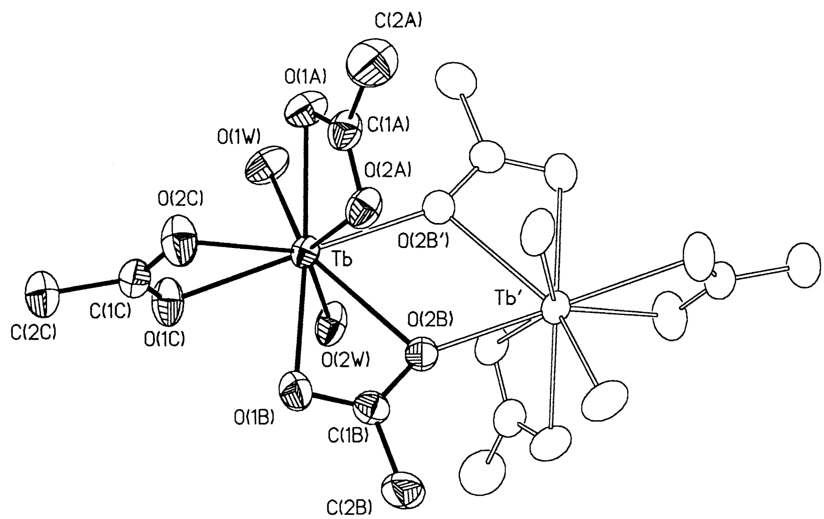

Fig. 1. XP plot of $[Tb_2(CH_3COO)_6(H_2O)_4]\cdot 4H_2O$ (**1**) with thermal ellipsoids at the 50% probability level. All hydrogen atoms have been omitted for clarity.

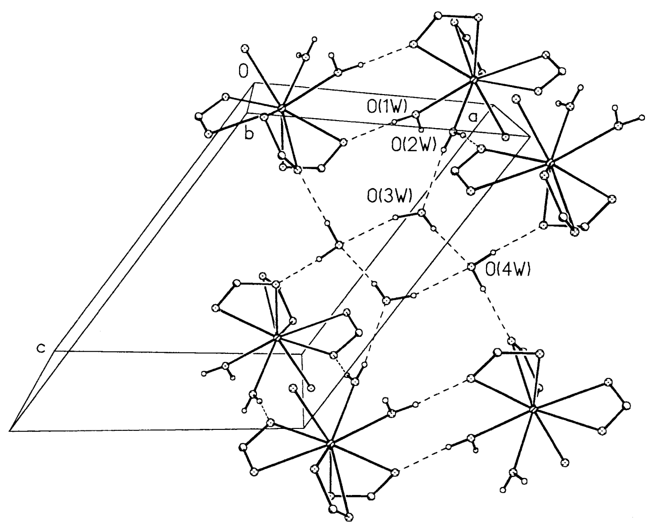

Fig. 2. Packing diagram for $[Tb_2(CH_3COO)_6(H_2O)_4]\cdot 4H_2O$ (**1**) along the crystallographic *b* axis (acetato is represented schematically). Hydrogen atoms not involved in H-bonding have been omitted for clarity.

suggesting a rather weak interaction between strips. This structure is isostructural to the reported for the gadolinium [29] and yttrium [30] analogues. For the slightly larger Eu(III) ion the isolated species under similar conditions has been found to be $[Eu(oda)(Hoda)(H_2O)]\cdot 2H_2O$ [14].

The crystal structure of **4** is built up from two distinct types of building blocks, TbO_9 and CuO_6 as illustrated in Figs. 7 and 8. It is isostructural to the other members of the series $[\{Cu_3Ln_2(oda)_6(H_2O)_6\}\cdot 12H_2O]_n$ given in Ref. [17], where a detailed discussion of the structure can be found. Non-bonded distances are Tb···Cu = 5.683(1), Cu···Cu = 7.346(1) and Tb···Tb = 7.563(1) Å.

Table 3
Hydrogen bonding in compounds **1**–**4** [a]

O–H···O	O–H (Å)	H···O (Å)	O···O (Å)	O–H···O (°)
1				
O4W–H4WB···O2C	0.85(5)	1.91(5)	2.759(4)	173(4)
O4W–H4WA···O1B^{i}	0.81(6)	1.93(6)	2.733(4)	178(5)
O3W–H3WB···O4W^{ii}	0.76(5)	2.05(5)	2.801(5)	174(5)
O3W–H3WA···O4W^{iii}	0.85(5)	2.05(5)	2.876(4)	164(5)
O2W–H2WB···O2A^{iv}	0.86(6)	1.92(6)	2.761(3)	164(5)
O2W–H2WA···O1C^{v}	0.76(6)	1.94(6)	2.700(3)	171(6)
O1W–H1WB···O3W^{vi}	0.65(4)	2.10(4)	2.737(5)	168(5)
O1W–H1WA···O1A^{vii}	0.85(6)	1.87(6)	2.713(4)	173(5)
2				
O1W–H1WA···O2B	0.76(3)	1.92(3)	2.647(4)	160(5)
O2W–H2WA···O2W^{viii}	0.77(3)	1.99(3)	2.758(4)	178(6)
O2W–H2WB···F3A$'^{ix}$	0.77(3)	2.28(4)	3.03(2)	167(8)
O3W–H3WA···O1C^{x}	0.77(3)	2.09(3)	2.845(3)	166(5)
O3W–H3WB···F3B$'^{x}$	0.76(2)	2.22(3)	2.961(12)	166(4)
O3W–H3WB···F3B$''^{x}$	0.76(2)	2.28(3)	3.029(16)	169(4)
3				
O2A–H2A···O4C^{xi}	0.90(3)	1.60(4)	2.483(9)	167(6)
O2B–H2B···O5A^{xi}	0.88(4)	1.94(6)	2.643(11)	136(6)
O2B–H2B···O4A^{xi}	0.88(4)	2.11(6)	2.896(13)	148(6)
O2C–H2C···O5B^{xi}	0.89(3)	1.72(4)	2.596(8)	164(6)
O2D–H2D···O4B^{xi}	0.87(3)	1.77(4)	2.618(9)	164(6)
O4D–H4D···O1W^{xii}	0.88(3)	1.70(3)	2.578(10)	173(7)
O1W–H1WA···O5D^{xiii}	0.88(4)	2.34(5)	2.883(11)	120(11)
O1W–H1WB···O3D	0.88(4)	2.45(6)	2.984(10)	120(10)
O1W–H1WB···O5D	0.88(4)	2.24(6)	3.056(10)	154(11)
4				
O1W–H1W···O1^{xiv}	0.90(4)	1.92(4)	2.790(3)	163(4)

[a] Symmetry codes: (i) $-x+1, -y+2, -z+1$; (ii) $x+1, y, z$; (iii) $-x+1, -y+1, -z+1$; (iv) $-x, -y+2, -z$; (v) $-x+1, -y+2, -z$; (vi) $-x+1, -y+1, -z$; (vii) $-x, -y+1, -z$; (viii) $x, -y+1/2, z-1/2$; (ix) $x-1, y, z-1$; (x) $-x, -y+1, -z+1$; (xi) $x+1, y, z$; (xii) $x-1, y, z$; (xiii) $-x+1, -y, -z+2$; (xiv) $x, y, -z$.

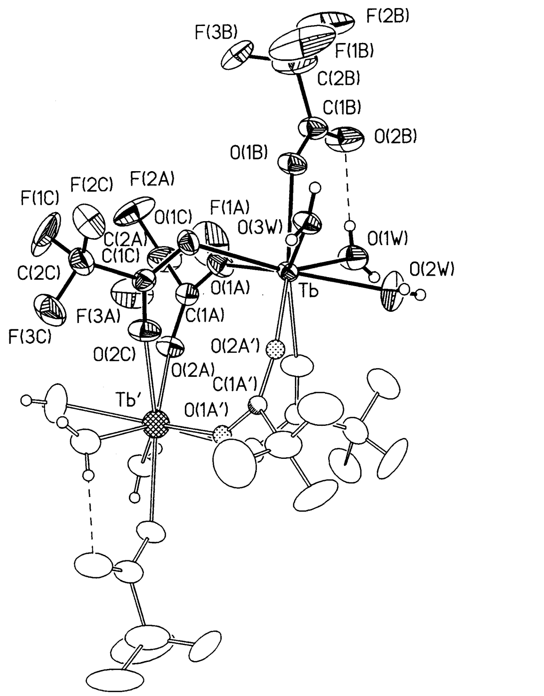

Fig. 3. XP plot of $[Tb_2(CF_3COO)_6(H_2O)_6]$ (**2**) with thermal ellipsoids at the 50% probability level. All hydrogen atoms have been omitted for clarity.

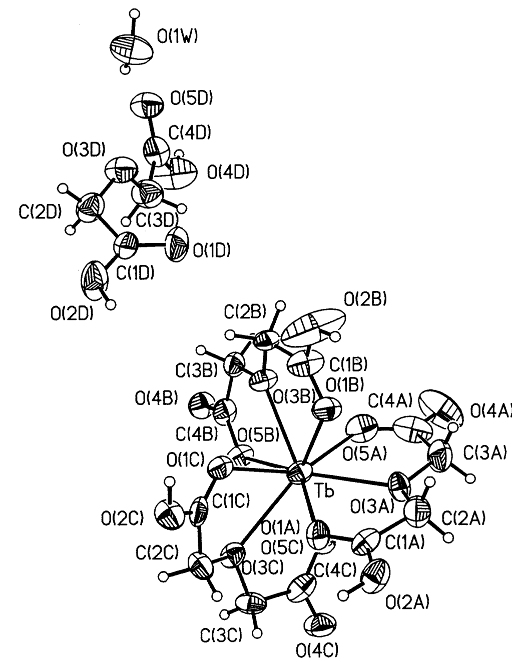

Fig. 5. XP plot of $[Tb(Hoda)_3]\cdot H_2oda\cdot H_2O$ (**3**) with thermal ellipsoids at the 50% probability level.

3.2. Magnetic properties of **4**

The magnetic behavior of the heterometallic Cu–Tb compound **4** is represented in Fig. 9 in the form of the thermal dependence of the $\chi_M T$ product, where χ_M is the magnetic susceptibility per Tb_2Cu_3 unit. Experimental data were obtained in the range 2–300 K under an applied field of 500 G. The $\chi_M T$ value at room temperature is equal to 23.44 emu K mol^{-1}, which is close to the sum of the values for three Cu(II) and two Tb(III) free ions. Considering that in the isostructural Cu–Y compound, the three non-interacting Cu(II) ions have been shown to contribute 1.25 emu K mol^{-1} to the bulk value [17], it can be deduced from the total susceptibility and a magnetic moment of 9.60 μ_B per terbium atom is obtained. This value is close to the expected of 9.72 μ_B for an isolated non-interacting Tb(III) ion [31]. Fitting the data to the Curie–Weiss

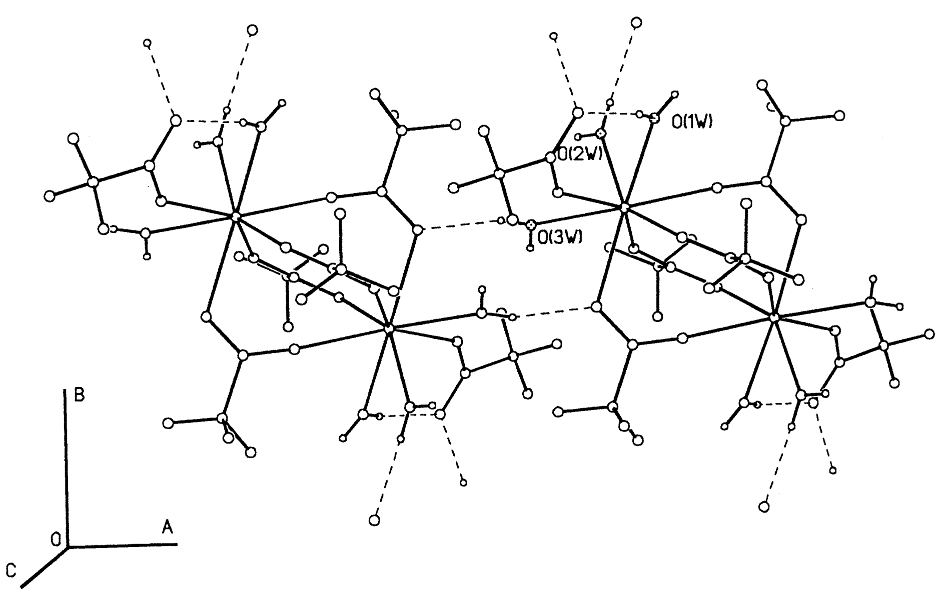

Fig. 4. Packing diagram for $[Tb_2(CF_3COO)_6(H_2O)_6]$ (**2**) showing the chains along the crystallographic *a* axis. Hydrogen atoms not involved in H-bonding have been omitted for clarity.

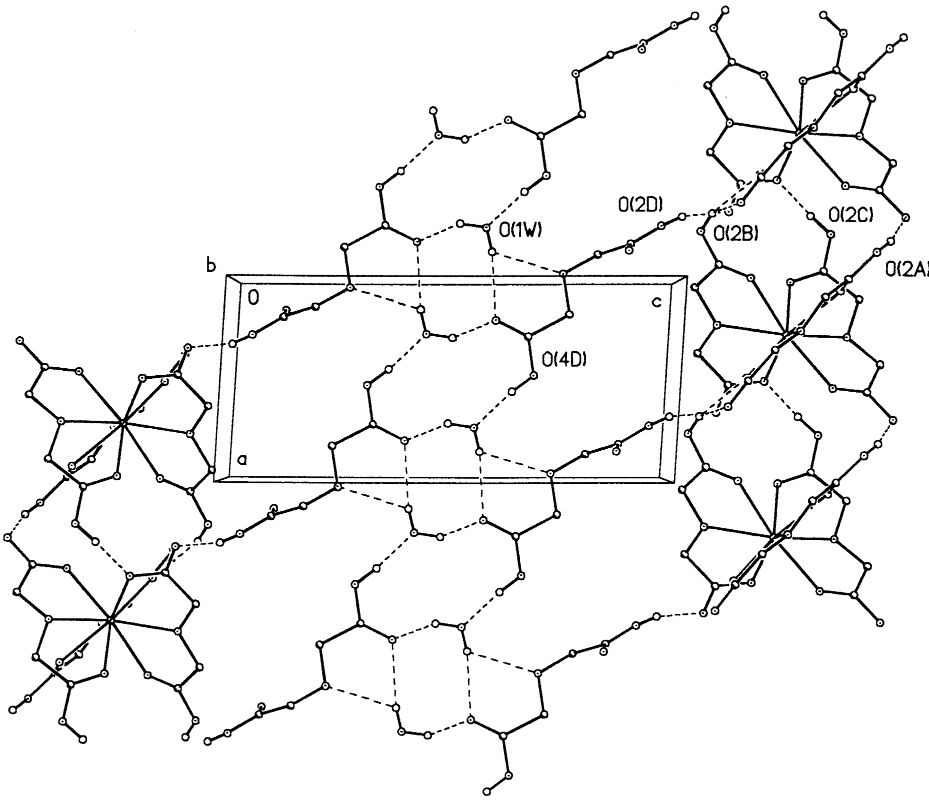

Fig. 6. Packing diagram for $[Tb(Hoda)_3]\cdot H_2oda\cdot H_2O$ (**3**) showing the broad solvent strip along the crystallographic *a* axis.

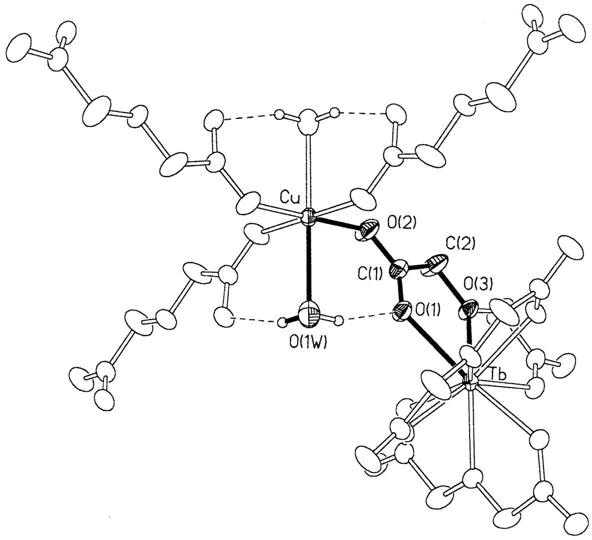

Fig. 7. XP plot showing the building unit of $[\{Cu_3Tb_2(oda)_6(H_2O)_6\}\cdot 12H_2O]_n$ (**4**) with thermal ellipsoids at the 50% probability level.

law in the range 40–300 K gave a θ value of -8.5 K, indicative of an antiferromagnetic behavior. The profile of Fig. 9 shows that $\chi_M T$ decreases upon cooling, the lower the temperature, the quicker the decrease. Comparison with the profile for the Cu–Y compound suggests that the sharp decrease of $\chi_M T$ observed at low temperatures (below 50 K), should mainly arise from the crystal field splitting of the Tb(III) ions. No information can be extracted at this point on the nature of the Cu–Tb interactions in the system.

3.3. Luminescent properties

The luminescence emission spectra of powder samples and of aqueous solutions of compounds **1**, **2** and **3** were recorded. The spectra of compounds **1** and **2** are nearly identical, consequently only those for **1** and **3** are shown in Figs. 10 and 11, respectively. The characteristic Tb(III) metal centered transition bands ($^5D_4 \rightarrow {}^7F_J$) are observed at 488, 543, 583 and 621 nm for $J = 6$, 5, 4 and 3, respectively.

It is known that the quenching of the luminescence of lanthanide cations in aqueous solution occurs through energy transfer from the electronic excited state of the metal ion into the O–H vibrational overtones of the coordinated water molecules. The number of these, q, can be derived from the first order decay rate constants of the lanthanide complexes in H_2O (k_{H2O}) and in D_2O (k_{D2O}), as described in the literature [32–34]. The emission lifetimes registered at 488 and at 544 nm for compounds **1** and **3** in H_2O and D_2O used to derive the q values, are given in Table 4. Mean values for k_{H2O} and k_{D2O} in ms^{-1} were used in the calculations. The q values obtained by Horrocks' relationship [33] ($q = 4.2\Delta k$) are 8.4 for **1** and 3.3 for **3**. The former indicates the presence

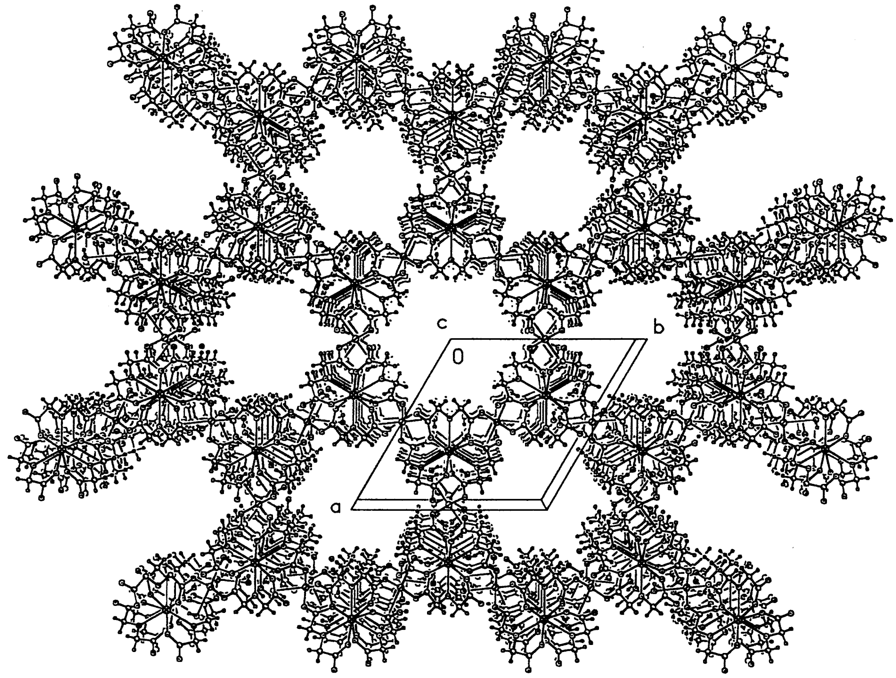

Fig. 8. Packing view of $[\{Cu_3Tb_2(oda)_6(H_2O)_6\}\cdot 12H_2O]_n$ (**4**) showing the highly connected 3D columnar structure generated, as well as the channels along the crystallographic c axis.

of $[Tb(H_2O)_9]^{3+}$ as the predominant species in solution, as reported for other aquo complexes of Tb(III). The value $q = 3.3$ for **3** is consistent with the assumption that water molecules may substitute various coordination sites of tridentate Hoda in the $[Tb(Hoda)_3]$ species. We note that values of $q = 2.9$ were reported for the Tb(III) EDTA system in aqueous solution.

Heavy metal cations may also quench the luminescence of the lanthanide ions in aqueous solution, although the mechanism has not been well established [35,36]. We measured the emission decay constants of **1** and **3** in the presence of variable amounts of Cu(II) in aqueous solution, obtaining values of 2×10^6 and 8×10^6 M^{-1} s^{-1}, respectively, for the dynamic deactivation rate constant k_Q obtained from linear Stern–Volmer plots. The simultaneous presence of two positive species, $[Tb(H_2O)_9]^{3+}$ and Cu(II) in the aqueous solution of **1** is likely to reduce the quenching effect, as evidenced by the lower constant in Table 4. In solid compound **4**, the metal centered emission of Tb(III) is completely

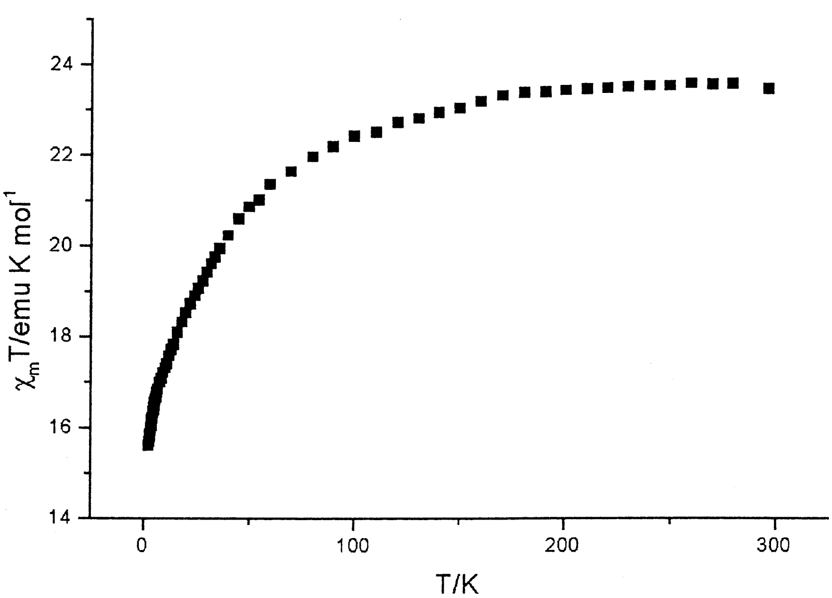

Fig. 9. Plot of $\chi_M T$ vs. T for compound $[\{Cu_3Tb_2(oda)_6(H_2O)_6\}\cdot 12H_2O]_n$ (**4**).

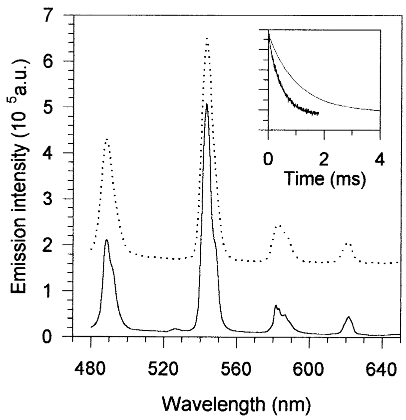

Fig. 10. Phosphorescence emission spectra for $[Tb_2(CH_3COO)_6(H_2O)_4]\cdot4H_2O$ (**1**) in solid state (full line) and in aqueous solution (dotted line). The inset shows the fluorescent decays of the solid (top) and of the aqueous solution (bottom).

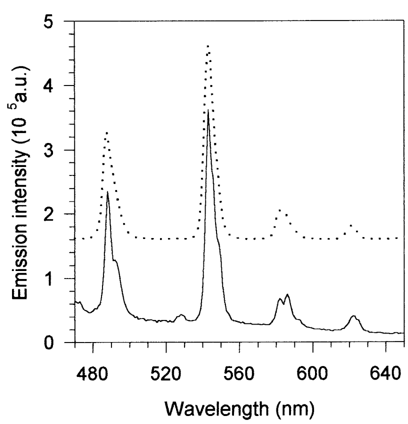

Fig. 11. Phosphorescence emission spectra for $[Tb(Hoda)_3]\cdot H_2oda\cdot H_2O$ (**3**) in solid state (full line) and in aqueous solution (dotted line).

Table 4
Emission lifetimes [a]

Compound	λ_{em} (nm)	τ (ms)	k (ms^{-1})
1 (solid)	544	1.03	0.97
	488	1.04	0.96
1 (in H_2O)	544	0.42	2.41
	488	0.43	2.34
1 (in D_2O)	544	2.86	0.35
	488	2.64	0.38
3 (in H_2O)	545	0.98	1.02
	488	1.00	1.00
3 (in D_2O)	545	4.33	0.23
	488	4.15	0.24
4 (in H_2O)	545	0.056	18

[a] All solutions were measured at a 2–3 mM concentration. Typical error in lifetime measurements is $\pm10\%$.

quenched at room temperature. A similar behavior has been recently reported for Eu(III) in $[CuEu_2(CCl_3COO)_8]\cdot6H_2O$ at 293 and at 77 K [37]. The emission decay time of the polymer was also measured in a 2 mM aqueous solution and a value of 17.8 ms^{-1} ($\tau = 52$ μs) was obtained for the decay rate constant, Table 4. This low value is due to the non-radiative deactivating process of the Cu(II) ion.

In conclusion: (i) three terbium carboxylates are structurally characterized showing a variety of combinations of coordination and H-bonds; (ii) the nature of the main species of the terbium carboxylates in solution is derived from photoluminescence measurements; and (iii) a microporous polymer containing Cu_3Tb_2 clusters bonded by oxydiacetates is structurally characterized, it shows antiferromagnetic behavior and complete quenching of the luminescence.

4. Supplementary material

X-ray crystallographic files in CIF format for compounds **1**–**4** have been deposited with the Cambridge Crystallographic Data Center, CCDC Nos. 190673–190676 for structures **1**–**4**, respectively. Copies of this information may be obtained free of charge from The Director, CCDC, 12 Union Road, Cambridge, CB2 1EZ, UK (fax: +44-1223-336-033; e-mail: deposit@ccdc.cam.ac.uk or www: http://www.ccdc.cam.ac.uk).

Acknowledgements

This work was supported by Fundacion Andes C-13575, CONICYT FONDAP 11980002, PICS 922, FONDECYT 1020802 (Chile) and ANPCyT-PICT4438 and CONICET-PIP0388 (Argentina). P.F.A. and M.P. are members of CONICET.

References

[1] C. Mehrotra, R. Bohra, Metal Carboxylates, New York, Academic Press, 1983.
[2] A. Ouchi, Y. Suzuki, Y. Ohki, Y. Koizumi, Coord. Chem. Rev. 92 (1988) 29.
[3] Gmelin Handbook of Inorganic Chemistry, Sc, Y, La-Lu Carboxylates, D5, Springer, New York, 1984.
[4] F.A. Hart, in: G. Wilkinson, R.D. Gillard, J.A. McCleverty (Eds.), Comprehensive Coordination Chemistry, vol. 3 (Chapter 38), Pergamon, Oxford, 1987.
[5] T.M. Reineke, M. Eddaoudi, M. Fehr, D. Kelly, O.M. Yaghi, J. Am. Chem. Soc. 121 (1999) 1651.
[6] L. Ma, O.R. Evans, B.M. Foxman, W. Lin, Inorg. Chem. 38 (1999) 5837.
[7] J.S. Seo, D. Whang, H. Lee, S.I. Jun, J. Oh, Y.J. Jeon, K. Kim, Nature 404 (2000) 982.

[8] J. Ballato, J.S. Lewis, III, P. Holloway, Mater. Res. Soc. Bull. 24 (1999) 51.
[9] J.-C.G. Bünzli, in: G.R. Chopin, J.-C.G. Bünzli (Eds.), Lanthanide Probes in life, Chemical and Earth Sciences (Chapter 7), Elsevier Science, Amsterdam, 1989.
[10] S. Wang, Z. Pang, K.D.L. Smith, M.J. Wagner, J. Chem. Soc., Dalton Trans. (1994) 955.
[11] Y. Yansheng, L. Lubin, T.C.W. Mak, Chin. J. Struct. Chem. (Jiegou Huaxue) 7 (1988) 1.
[12] S. Ganapathy, V.P. Chacko, R.G. Bryant, M.C. Etter, J. Am. Chem. Soc. 108 (1986) 3159.
[13] E.S. Panin, V.Ya. Kavun, V.I. Sergienko, B.V. Butvetskii, Koord. Him. 11 (1985) 1539.
[14] P.F. Aramendia, R. Baggio, M.T. Garland, M. Perec, Inorg. Chim. Acta 303 (2000) 306.
[15] P. Pascal, Ann. Chim. Phys. 19 (1910) 5.
[16] Powder Diffraction File 13-387, JCPDS. International Center for Diffraction Data, Newtown Square, PA, 1992.
[17] R. Baggio, M.T. Garland, Y. Moreno, O. Peña, M. Perec, E. Spodine, J. Chem. Soc., Dalton Trans. (2000) 2061.
[18] R. Baggio, M.T. Garland, M. Perec, Inorg. Chem. 36 (1997) 950.
[19] G.M. Sheldrick, SHELXL-97: Program for Crystal Structure Refinement, University of Göttingen, Göttingen, Germany, 1997.
[20] G.M. Sheldrick, XP in SHELXL-PC, Version 4.2, Siemens Analytical X-ray Instruments Inc., Madison, WI, 1991.
[21] Y. Yansheng, L. Lubin, T.C.W. Mak, Chin. J. Struct. Chem. 7 (1988) 1.
[22] M.C. Favas, D.L. Kepert, B.W. Skelton, A.H. White, J. Chem. Soc., Dalton Trans. (1980) 454.
[23] J.W. Bats, R. Kalus, H. Fuess, Acta Crystallogr., B 35 (1979) 1225.
[24] H. Sawase, Y. Koizumi, Y. Suzuki, M. Shimoi, A. Ouchi, Bull. Chem. Soc. Jpn. 57 (1984) 2730.
[25] S.P. Bone, D.B. Sowerby, R.D. Verma, J. Chem. Soc., Dalton Trans. (1978) 1544.
[26] V.Ya. Kavun, T.A. Kaidalova, V.I. Kostin, E.S. Panin, B.N. Chemyshov, Koord. Him. 10 (1984) 1502.
[27] J. Zhang, S. Zhang, M. Xiuqin, W. Gecheng, H. Ninghai, J. Zhongsheng, Chin. J. Appl. Chem. 5 (1988) 30.
[28] G.V. Romanenko, S.P. Sokolova, S.V. Lanionov, Zh. Struct. Him. 40 (1999) 387.
[29] R. Baggio, M.T. Garland, M. Perec, Inorg. Chem. 30 (1997) 950.
[30] R. Baggio, M.T. Garland, M. Perec, Inorg. Chim. Acta 281 (1998) 18.
[31] O. Kahn, Molecular Magnetism, VCH, Weinheim, 1993.
[32] D. Parker, G. Williams, J. Chem. Soc., Dalton Trans. (1996) 3613.
[33] W.D. Horrocks, D.R. Sudnick, J. Am. Chem. Soc. 101 (1979) 334.
[34] A. Beeby, I.M. Clarkson, R.S. Dickins, S. Faulkner, D. Parker, L. Royle, A.S. de Sousa, J.A.G. Williams, M. Woods, J. Chem. Soc., Perkin Trans. 2 (1999) 493.
[35] M.A. Kessler, Anal. Chim. Acta 364 (1998) 125.
[36] M. Berton, F. Mancin, G. Stocchero, P. Tecila, U. Tonellato, Langmuir 17 (2001) 7521.
[37] J. Legendziewicz, M. Borzechowska, J. Alloys Compd. 300–301 (2000) 353.